C–H Bond Activation

DOI: 10.1002/anie.201001850

Analysis of Reaction Channels for Alkane Hydroxylation by Nonheme Iron(IV)–Oxo Complexes**

*Caiyun Geng, Shengfa Ye, and Frank Neese**

Ever since the discovery of xenobiotic degradation by cytochrome P450,[1] the functionalization of unactivated C–H bonds has been a focal point of experimental and theoretical research. Except for the well-accepted iron(IV)–oxo intermediate, which presumably is the active species in cytochrome P450 as well as in some nonheme iron enzymes,[1–2] iron(V)–oxo[2c,3] or iron(III)–hydroperoxo[4] intermediates might also be involved in C–H bond hydroxylation reactions. Such open-shell transition metals in high oxidation states display fascinating and highly complex reactivity patterns. The pioneering work by Shaik, Schwarz, and co-workers on the gas-phase reaction of FeO^+ with H_2 has laid out the concept of two-state reactivity as an important motif in transition-metal oxidation chemistry.[5] It has been shown that reaction barriers may differ dramatically on potential energy surfaces that are characterized by different spin multiplicities, and that the system may employ more than one such surface during the reaction.[6] Much progress has been made in the synthetic modeling of iron(IV)–oxo species.[2c,7] Moreover, quantum chemical studies by Solomon,[4b,8] Thiel,[9] Shaik,[6,10] Siegbahn,[11] Baerends,[12] de Visser[13] and their co-workers have provided a framework for the mechanistic analysis of C–H bond hydroxylation by both heme and nonheme iron(IV)–oxo complexes. A detailed mechanistic understanding of the reactivity displayed by iron(IV)–oxo centers is a prerequisite for the rational design of low molecular weight catalysts.

The pioneering proposal by Groves and McClusky suggests that the alkane hydroxylation reaction using iron(IV)–oxo intermediates follows a rebound mechanism.[14] The overall mechanism in rebound chemistry is characterized by two steps: 1) hydrogen-atom abstraction from the substrate R–H via transition state $\mathbf{TS_H}$ that leads to a iron(III)–hydroxyl species that is weakly bound to an alkyl radical R· (intermediate I), and 2) hydroxyl back-transfer to the radical R· via transition state $\mathbf{TS_{Re}}$ to yield an iron(II) centre and the hydroxylated product, R–OH.

However, there are two additional layers of complexity. First, iron(IV)–oxo sites are known to exist either in triplet or quintet ground states. The majority of model complexes prefer the former,[7] whereas all of the identified nonheme iron enzyme active sites[2b] feature the latter. More recently, model complexes with an $S=2$ ground state have been synthesized.[15] From density functional theory (DFT) calculations, the reactivity of quintet iron(IV)–oxo intermediates towards C–H bond hydroxylation is suggested to be much higher than the corresponding triplet species.[6b,10a,d,16] The second layer of complexity stems from the geometry of the substrate approach. The cleaving C–H bond may attack the iron(IV)–oxo unit either from the top (thus leading to an essentially linear Fe-O-H arrangement), or from an equatorial position (thus leading to a bent Fe-O-H geometry). Both types of reaction geometries lead to different electronic structures in the transition states and hence to different reaction pathways.

The initial step of hydrogen-atom abstraction involves the transfer of one electron from the substrate into the metal 3d-block. This step is already electronically complicated because it has been established that a preparatory step is needed—in which the system switches from an iron(IV)–oxo to an iron(III)–oxyl species on its way towards the transition state.[16] Obviously, depending on the ground state multiplicity

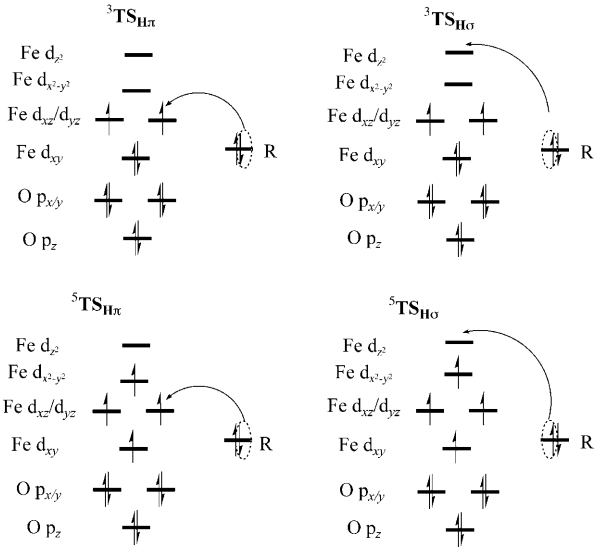

Scheme 1. The feasible reaction channels for the hydrogen-atom abstraction by iron(IV)–oxo complexes.

[*] C. Geng, Dr. S. Ye, Prof. Dr. F. Neese
Institut für Physikalische und Theoretische Chemie
University of Bonn
Wegelerstrasse 12, 53115 Bonn (Germany)
Fax: (+49) 228-73-9064
E-mail: neese@thch.uni-bonn.de
Homepage: http://www.thch.uni-bonn.de/tc/
C. Geng
State Key Laboratory of Theoretical and Computational Chemistry
Institute of Theoretical Chemistry, Jilin University
Changchun 130023 (China)

[**] This work was supported by the China Scholarship Council (CSC) (C.Y.G.). S.Y. and F.N. gratefully acknowledge a grant from the German Science Foundation (NE 690/7-1).

Supporting information for this article is available on the WWW under http://dx.doi.org/10.1002/anie.201001850.

© 2010 Wiley-VCH Verlag GmbH & Co. KGaA, Weinheim

and the geometry of the C–H bond approach, several of the semi-occupied or unoccupied iron-based molecular orbitals could serve as electron acceptors. In the quintet channel (Scheme 1, bottom right panel), the electron of the substrate is transferred into the σ*(FeO) antibonding orbital (σ-mechanism). The upwards pointing lobe of the O p_z orbital requires a vertical approach of the substrate and hence ^{5}**TS$_{H\sigma}$** features a nearly collinear Fe-O-H arrangement. In the triplet pathway (Scheme 1, top left panel), the π*(FeO) orbital accepts the electron from the substrate C–H bond (π-mechanism). The corresponding transition state ^{3}**TS$_{H\pi}$** is characterized by a bent Fe-O-H unit to accomplish maximum orbital overlap between the electron-donor and -acceptor orbitals. In the rebound step, the C–O bond formation is accompanied by a simultaneous electron transfer from the substrate into the Fe $d_{xz/yz}$ and the vacant Fe d_{z^2} orbitals, respectively. Thus, the rebound step appears to follow a π-mechanism on the quintet surface and a σ-mechanism on the triplet surface.

Despite this already detailed understanding that has been reached through intense experimental and theoretical studies, the picture is not yet complete. A recent study by Solomon and co-workers[17] on the benzylic hydroxylation of (4-hydroxy)mandelate synthase (HmaS) revealed a new reaction pathway on the quintet surface (Scheme 1, bottom left panel). Here, the benzylic hydrogen atom approaches the electrophilic Fe–O moiety in a horizontal fashion. This approach leads to the transfer of a β- rather than an α-spin electron into the π*(FeO) orbital, similar to what is commonly observed for the triplet π-pathway discussed above. Thus, this study is the first one to propose a π-mechanism for hydrogen-atom transfer to an iron(IV)–oxo center on the quintet surface. However, this new channel might be regarded as a special case. First, the substrate is directly coordinated to the iron active site and hence steric encumbrance restricts it to a horizontal approach. Second, the reaction involves the abstraction of a benzylic hydrogen atom that is much weaker than the aliphatic C–H bonds activated by cytochrome P450 or other nonheme iron centers.

We are therefore interested in the question of whether the quintet π-pathway is a generally competitive reaction channel for alkane hydroxylation and whether a σ-pathway is also possible on the triplet surface (Scheme 1, top right panel). To this end, we have studied all four possible reaction channels with the aid of DFT calculations as well as with high-level coupled cluster theory with single, double, and triple excitations (CCSD(T); see the Supporting Information for computational details). The chosen models resembled those previously investigated for property correlations among high-valent iron centers: $[Fe^{IV}(O)(NH_3)_5]^{2+}$ (**a**), $[Fe^{IV}(O)(OH)_{(axial)}(NH_3)_4]^{+}$ (**b**), $[Fe^{IV}(O)(OH)_{2(eq)}(NH_3)_3]$ (**c**). The calculated geometric parameters of the transition states of the $[Fe^{IV}(O)(NH_3)_5]^{2+}$ system (Table 1) agree well with previous results of the same pathways.[10a,c,12b,18]

We first discuss the hydroxylation reactions based on the DFT calculations. Figure 1 shows the potential energy profiles of the ethane C–H bond hydroxylation by model system **a**. The processes that proceed through ^{3}**TS$_{H\pi}$** and ^{5}**TS$_{H\sigma}$** represent the established pathways on the triplet and quintet surfaces. The reactions proceeding via ^{3}**TS$_{H\sigma}$** and ^{5}**TS$_{H\pi}$** are the nonclassical reactions. The triplet and quintet iron(IV)–oxo reactants have very similar energies, which is consistent with previous studies.[10a,c,13b] Comparison of the calculated energy barriers for hydrogen-atom abstraction demonstrates that the quintet σ-pathway encounters by far the lowest barrier among the four alternatives. In contrast, the π-pathways on the triplet and quintet surfaces have comparable energy barriers. The barrier of the triplet σ-pathway, which could only be located for model system **a**, is much higher in energy. For the rebound step, the triplet pathway involves a higher energy barrier than the quintet pathway. Hence, it is clear that the hydroxylation reactivity decreases in the order $^5\sigma > {}^5\pi > {}^3\pi > {}^3\sigma$. Apart from the nonclassical channels discussed here, our results are in agreement with previous studies[11–,12d,13a] that demonstrate that the quintet iron(IV)–oxo species is more reactive than the corresponding triplet species.

As the electron-transfer steps in the established triplet (π-mechanism) and quintet (σ-mechanism) reaction pathways have been well studied, our discussion will mainly focus on the π-mechanism on the quintet state surface and the σ-pathway on the triplet state. For simplicity, we focus the discussion on model system **a** and have collected the analo-

Table 1: Geometric parameters of the transition states of the $[Fe^{IV}(O)(NH_3)_5]^{2+}$ system calculated at the B3LYP/TZVP level of theory.

Transition states	Fe–O [Å]	O–H [Å]	C–H [Å]	C–O [Å]	∡FeOH [°]	∡FeOC [°]
^{3}**TS$_{H\pi}$**	1.78	1.21	1.33	–	118.9	–
^{3}**TS$_{H\sigma}$**	1.78	1.16	1.37	–	174.9	–
^{5}**TS$_{H\sigma}$**	1.74	1.27	1.26	–	175.8	–
^{5}**TS$_{H\pi}$**	1.76	1.21	1.33	–	123.1	–
^{3}**TS$_{Re\sigma}$**	1.91	0.97	–	2.27	–	160.0
^{5}**TS$_{Re\pi}$**	–	–	–	–	–	–
^{5}**TS$_{Re\sigma}$**	1.84	0.97	–	2.79	–	174.7

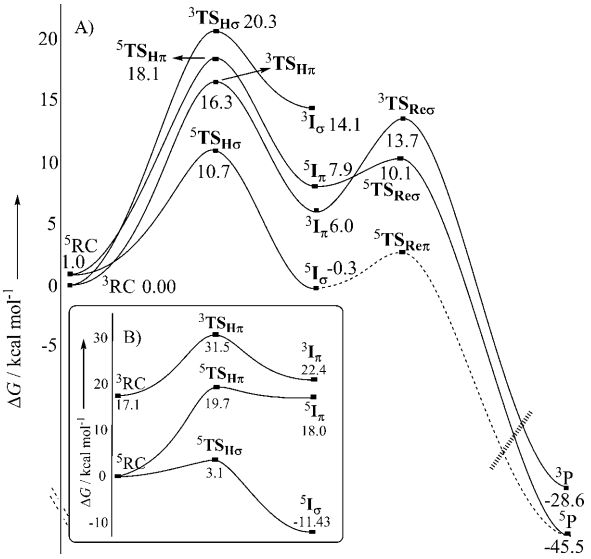

Figure 1. Schematic Gibbs free energy (ΔG) surfaces for ethane hydroxylation by the $[Fe^{IV}(O)(NH_3)_5]^{2+}$ system: A) B3LYP/def2-TZVPP//B3LYP/TZVP, B) CCSD(T) (def2-TZVP for Fe, N, O, and def2-SV(P) for H atoms)//B3LYP/TZVP.

 © 2010 Wiley-VCH Verlag GmbH & Co. KGaA, Weinheim

gous results for model systems **b** and **c** in the Supporting Information. Figure 2 shows the schematic molecular orbital (MO) diagrams for the two nonclassical pathways. It becomes evident that in $^5\mathbf{TS}_{\mathbf{H}\pi}$ a β-electron from the substrate is shifted towards the Fe-d_{xz} based orbital, which is consistent with a horizontal approach of the ethane molecule towards the Fe–O moiety. The key geometric parameters of $^5\mathbf{TS}_{\mathbf{H}\pi}$ closely resemble those found in $^3\mathbf{TS}_{\mathbf{H}\pi}$ (Table 1), that is, a nearly collinear O-H-C moiety, comparable C–H and O–H bond lengths and a significantly bent Fe-O-H angle. These findings may be rationalized by reference to the electronic configuration of $^5\mathbf{TS}_{\mathbf{H}\pi}$. As the substrate approaches the iron(IV)–oxo unit, the Fe–O bond gradually elongates and an electron hole is generated in the orbital based on O p_x[17] (thus leading to the formation of a ferric–oxyl species), which finally serves as the true electron acceptor. To assure the best orbital interactions between the C–H σ-bond and the O p_x orbital, the substrates must approach the FeO core horizontally with a Fe-O-H angle of 90°; however, this orientation is only possible at the expense of a much larger Pauli repulsion than in the σ-type attack geometry.[12c] Consequently, the opposing requirements of optimal orbital overlap and increasing Pauli repulsion lead to bent geometries in $^5\mathbf{TS}_{\mathbf{H}\pi}$ with a Fe-O-H angle close to 120°. Compared to the decreased Pauli repulsion and the optimum orbital interaction of the vertical approach in the quintet σ-mechanism, one may readily appreciate why $^5\mathbf{TS}_{\mathbf{H}\sigma}$ features the smallest barrier of the three pathways ($^5\mathbf{TS}_{\mathbf{H}\sigma}$, $^5\mathbf{TS}_{\mathbf{H}\pi}$, and $^3\mathbf{TS}_{\mathbf{H}\pi}$). Unlike $^5\mathbf{I}_\sigma$, which contains a high-spin ferric ion ($S_{Fe}=5/2$) that is antiferromagnetically coupled to an alkyl radical ($S_C=1/2$), the hydrogen-atom abstraction process through the π-mechanism finally leads to an intermediate ($^5\mathbf{I}_\pi$) containing an intermediate spin iron(III)–hydroxo complex ($S_{Fe}=3/2$) ferromagnetically coupled to an ethylic radical.

The vertical approach of ethane towards the Fe–O moiety in $^3\mathbf{TS}_{\mathbf{H}\sigma}$ leads to an α-electron transfer from the substrate to the σ*(FeO) antibonding orbital. Although the nearly collinear arrangement of Fe-O-H-C features the best orbital interactions and smallest Pauli repulsions, the LUMO + 1 acceptor orbital σ*(FeO) is much higher in energy compared to the corresponding orbital in $^5\mathbf{TS}_{\mathbf{H}\sigma}$ owing to the greatly reduced spin polarization.[8] The high activation energy of $^3\mathbf{TS}_{\mathbf{H}\sigma}$ is also in agreement with the geometric parameters that indicate a rather "late" transition state. The electronic structure of $^3\mathbf{I}_\sigma$ features antiferromagnetic coupling between an intermediate spin ferric ($S_{Fe}=3/2$) and an alkyl radical ($S_C=1/2$). The energies of these four intermediates of varying spin multiplicities decrease in the order $^5\mathbf{I}_\sigma$ ($S_{Fe}=5/2$) > $^5\mathbf{I}_\pi$ ($S_{Fe}=3/2$) ≥ $^3\mathbf{I}_\pi$ ($S_{Fe}=1/2$) > $^3\mathbf{I}_\sigma$ ($S_{Fe}=3/2$), which is consistent with the weak ligand fields arising from typical nonheme ligand frameworks.

Starting from $^5\mathbf{I}_\pi$, the rebound step follows a σ-mechanism through $^5\mathbf{TS}_{\mathbf{Re}\sigma}$ like in the triplet π-channel. In either case, the remaining α-electron of the substrate radical is transferred to the strongly σ-antibonding Fe d_{z^2} orbital (a schematic MO diagram of a post-$^5\mathbf{TS}_{\mathbf{Re}\sigma}$ geometry with a C–O bond length of 2.5 Å is shown in Figure 2C). As the electron is shifted along the Fe–O axis, an almost linear Fe-O-C angle of 174.7° is calculated in $^5\mathbf{TS}_{\mathbf{Re}\sigma}$. Comparison of the rebound pathways reveals that the two channels on the quintet state surface[19]

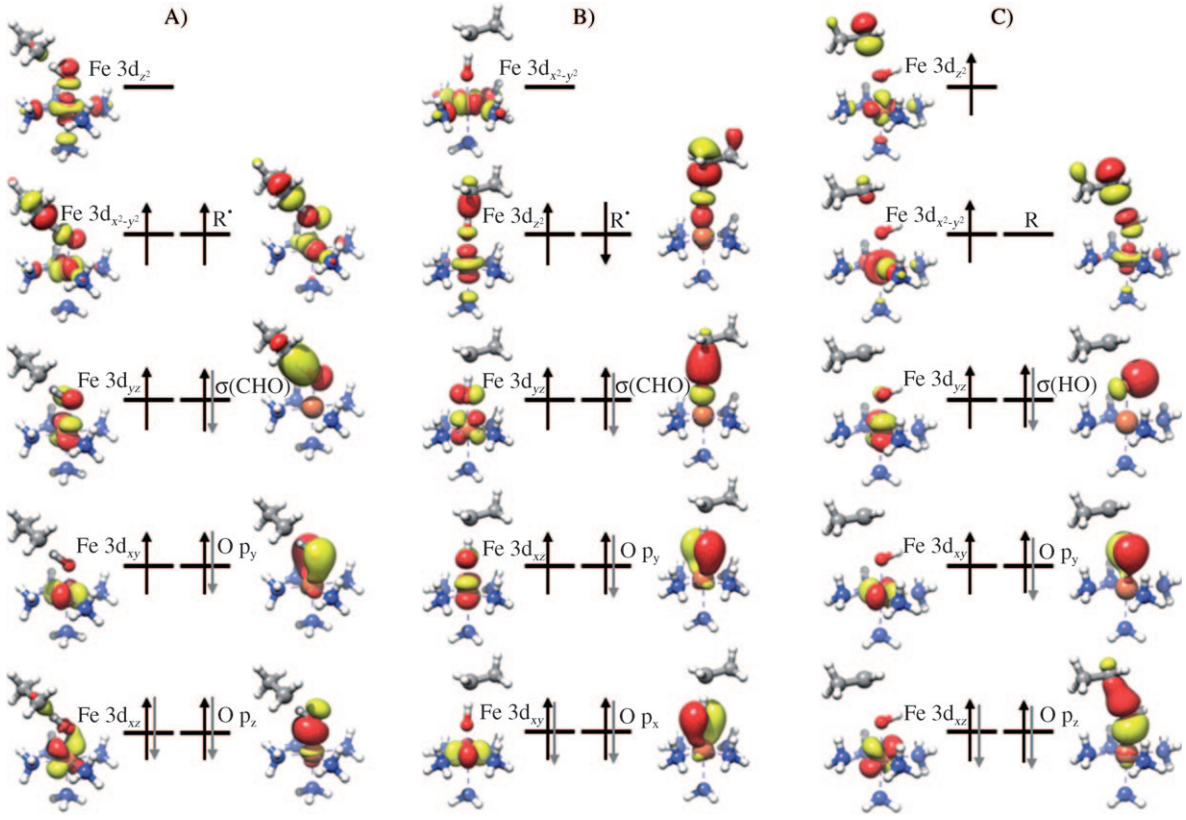

Figure 2. Schematic MO diagram of $^5\mathbf{TS}_{\mathbf{H}\pi}$ (A), $^3\mathbf{TS}_{\mathbf{H}\sigma}$ (B), and $^5\mathbf{TS}_{\mathbf{Re}\sigma}$ (C) for $[Fe^{IV}(O)(NH_3)_5]^{2+}$. C yellow, Fe orange, N blue, O red.

 © 2010 Wiley-VCH Verlag GmbH & Co. KGaA, Weinheim

have a very similar energy barrier, while the triplet σ-mechanism process encounters the highest energy barrier. This trend may be ascribed to two factors: 1) the nature of the electron-acceptor orbital, and 2) the spin polarization induced by the singly occupied orbitals in the metal d-block. Given the comparatively weak π-antibonding nature of the t_{2g}-derived orbitals compared to the strongly σ-antibonding nature of the orbital based on Fe d_{z^2} together with the large spin-polarization of the quintet state, it becomes understandable why $^5\mathbf{TS_{Re\pi}}$ corresponds to the lowest energy rebound step on the three surfaces. The situation on the triplet surface is exactly opposite. Here the acceptor orbital is the strongly σ-antibonding Fe d_{z^2} orbital and the triplet state spin-polarization is much less effective compared to the quintet state. An intermediate situation exists in $^5\mathbf{TS_{Re\sigma}}$.

The CCSD(T) level energies based on B3LYP optimized geometries predict larger triplet–quintet splitting patterns, which are again consistent with other studies (see the Supporting Information).[20] The CCSD(T) results are slightly biased in favor of the high-spin state of iron(IV)–oxo complexes. The same behavior is also found in the spectroscopic oriented configuration interaction (SORCI) calculations.[21] However, it is clear that there is a very large basis set dependence[22] and the basis set limit is difficult to reach with CCSD(T) calculations for systems of the present size. The activation energies obtained from CCSD(T) calculations for triplet and quintet pathways show a similar trend. In particular, the energy of $^5\mathbf{TS_{H\sigma}}$, which involves a high-spin ferric iron ($S_{Fe} = 5/2$), is greatly decreased. For the pathways involving intermediate-spin iron centers ($S_{Fe} = 3/2$), similar energy barriers as predicted by B3LYP calculations are obtained. This bias may disappear at the basis set limit, which is, unfortunately, not approachable with presently available computational resources. A detailed discussion of how to best obtain accurate spin-state energy gaps for transition metal complexes is beyond the scope of the present work. Nevertheless, the CCSD(T) results are broadly consistent with the B3LYP numbers for the hydrogen-atom abstraction steps, and further corroborate that the quintet σ-pathway is the most feasible channel. The CCSD(T) results also confirm that the quintet π-pathway is highly competitive.

In conclusion, this is the first time that all viable pathways have been identified in the same system, which allows us to compare their relative reactivities. The triplet σ-pathway is higher in energy such that it may not ever be involved in actual C–H bond hydroxylation reactions. However, the reactivity of the quintet π-channel is comparable or even higher than the classical triplet channel ($^3\boldsymbol{\pi}$), although it is slightly higher in energy than the established quintet channel ($^5\boldsymbol{\sigma}$). The existence of at least three energetically feasible pathways may offer, however, a new element of specificity control in C–H bond activation reactions by iron(IV)–oxo species. The choice of σ- or π-pathways could be controlled—at least in part—by steric hindrance in model systems or by the restrictions of the protein pocket in metalloenzymes.[8]

Received: March 29, 2010
Revised: May 11, 2010
Published online: July 13, 2010

Keywords: C–H activation · density functional calculations · iron–oxo species · reaction mechanisms

[1] *Cytochrome P450: Structure, Mechanism and Biochemistry*, 3rd ed. (Ed.: P. R. Ortiz de Montellano), Kluwer Academic/Plenum, New York, **2004**.
[2] a) E. I. Solomon, T. C. Brunold, M. I. Davis, J. N. Kemsley, S. K. Lee, N. Lehnert, F. Neese, A. J. Skulan, Y. S. Yang, J. Zhou, *Chem. Rev.* **2000**, *100*, 235; b) C. Krebs, D. G. Fujimori, C. T. Walsh, J. M. Bollinger, Jr., *Acc. Chem. Res.* **2007**, *40*, 484; c) M. Costas, M. P. Mehn, M. P. Jensen, L. Que Jr. , *Chem. Rev.* **2004**, *104*, 939.
[3] a) P. Comba, M. Maurer, P. Vadivelu, *J. Phys. Chem. A* **2008**, *112*, 13028; b) A. Bassan, M. R. A. Blomberg, P. E. M. Siegbalm, L. Que, Jr., *Chem. Eur. J.* **2005**, *11*, 692; c) K. Chen, L. Que, Jr., *J. Am. Chem. Soc.* **2001**, *123*, 6327; d) E. G. Kovaleva, J. D. Lipscomb, *Nat. Chem. Biol.* **2008**, *4*, 186.
[4] a) A. Decker, M. S. Chow, J. N. Kemsley, N. Lehnert, E. I. Solomon, *J. Am. Chem. Soc.* **2006**, *128*, 4719; b) E. I. Solomon, S. D. Wong, L. V. Liu, A. Decker, M. S. Chow, *Curr. Opin. Chem. Biol.* **2009**, *13*, 99.
[5] a) S. Shaik, M. Filatov, D. Schroder, H. Schwarz, *Chem. Eur. J.* **1998**, *4*, 193; b) D. Danovich, S. Shaik, *J. Am. Chem. Soc.* **1997**, *119*, 1773.
[6] a) S. Shaik, D. Kumar, S. P. de Visser, A. Altun, W. Thiel, *Chem. Rev.* **2005**, *105*, 2279; b) S. Shaik, H. Hirao, D. Kumar, *Acc. Chem. Res.* **2007**, *40*, 532.
[7] a) L. Que, Jr., *Acc. Chem. Res.* **2007**, *40*, 493; b) W. Nam, *Acc. Chem. Res.* **2007**, *40*, 522.
[8] A. Decker, J. Rohde, E. J. Klinker, S. D. Wong, L. Que, Jr., E. I. Solomon, *J. Am. Chem. Soc.* **2007**, *129*, 15983.
[9] J. C. Schöneboom, S. Cohen, H. Lin, S. Shaik, W. Thiel, *J. Am. Chem. Soc.* **2004**, *126*, 4017.
[10] a) H. Hirao, D. Kumar, L. Que, Jr., S. Shaik, *J. Am. Chem. Soc.* **2006**, *128*, 8590; b) S. Shaik, D. Kumar, S. P. de Visser, *J. Am. Chem. Soc.* **2008**, *130*, 10128; c) H. Hirao, L. Que, Jr., W. Nam, S. Shaik, *Chem. Eur. J.* **2008**, *14*, 1740; d) D. Kumar, H. Hirao, L. Que, Jr., S. Shaik, *J. Am. Chem. Soc.* **2005**, *127*, 8026.
[11] P. E. M. Siegbahn, T. Borowski, *Acc. Chem. Res.* **2006**, *39*, 729.
[12] a) L. Bernasconi, E. J. Baerends, *Eur. J. Inorg. Chem.* **2008**, 1672; b) L. Bernasconi, M. J. Louwerse, E. J. Baerends, *Eur. J. Inorg. Chem.* **2007**, 3023; c) C. Michel, E. J. Baerends, *Inorg. Chem.* **2009**, *48*, 3628; d) B. Ensing, F. Buda, M. C. M. Gribnau, E. J. Baerends, *J. Am. Chem. Soc.* **2004**, *126*, 4355.
[13] a) S. P. de Visser, *J. Am. Chem. Soc.* **2006**, *128*, 9813; b) S. P. de Visser, *J. Am. Chem. Soc.* **2006**, *128*, 15809; c) R. Latifi, M. Bagherzadeh, S. P. de Visser, *Chem. Eur. J.* **2009**, *15*, 6651.
[14] J. T. Groves, G. A. McClusky, *J. Am. Chem. Soc.* **1976**, *98*, 859.
[15] a) O. Pestovsky, S. Stoian, E. L. Bominaar, X. P. Shan, E. Munck, L. Que, Jr., A. Bakac, *Angew. Chem.* **2005**, *117*, 7031; *Angew. Chem. Int. Ed.* **2005**, *44*, 6871; b) J. England, M. Martinho, E. R. Farquhar, J. R. Frisch, E. L. Bominaar, E. Münck, L. Que, Jr., *Angew. Chem.* **2009**, *121*, 3676; *Angew. Chem. Int. Ed.* **2009**, *48*, 3622.
[16] S. Ye, F. Neese, *Curr. Opin. Chem. Biol.* **2009**, *13*, 89.
[17] M. L. Neidig, A. Decker, O. W. Choroba, F. Huang, M. Kavana, G. R. Moran, J. B. Spencer, E. I. Solomon, *Proc. Natl. Acad. Sci. USA* **2006**, *103*, 12966.
[18] J. F. Berry, S. Debeer. George, F. Neese, *Phys. Chem. Chem. Phys.* **2008**, *10*, 4361.
[19] S. Shaik, S. Cohen, S. P. de Visser, P. K. Sharma, D. Kumar, S. Kozuch, F. Ogliaro, D. Danovich, *Eur. J. Inorg. Chem.* **2004**, 207.
[20] A. Ghosh, E. Tangen, H. Ryeng, P. R. Taylor, *Eur. J. Inorg. Chem.* **2004**, 4555.
[21] F. Neese, *J. Inorg. Biochem.* **2006**, *100*, 716.
[22] a) N. Strickland, J. N. Harvey, *J. Phys. Chem. B* **2007**, *111*, 841; b) J. Oláh, J. N. Harvey, *J. Phys. Chem. A* **2009**, *113*, 7338.

 © 2010 Wiley-VCH Verlag GmbH & Co. KGaA, Weinheim